Cell Reports, Volume *44*

Supplemental information

Neuropeptide CRH prevents premature differentiation of OPCs following CNS injury and in early postnatal development

Clemens Ries, Tibor Stark, Benoit Boulat, Torben Ruhwedel, Jan Philipp Delling, Antonio Miralles Infante, Julia T. von Poblotzki, Alessandro Ulivi, Iven-Alex von Mücke-Heim, Simon Chang, Kenji Sakimura, Keiichi Itoi, Dennis B. Nestvogel, Alessio Attardo, Michael Czisch, Klaus-Armin Nave, Wiebke Möbius, Leda Dimou, and Jan M. Deussing

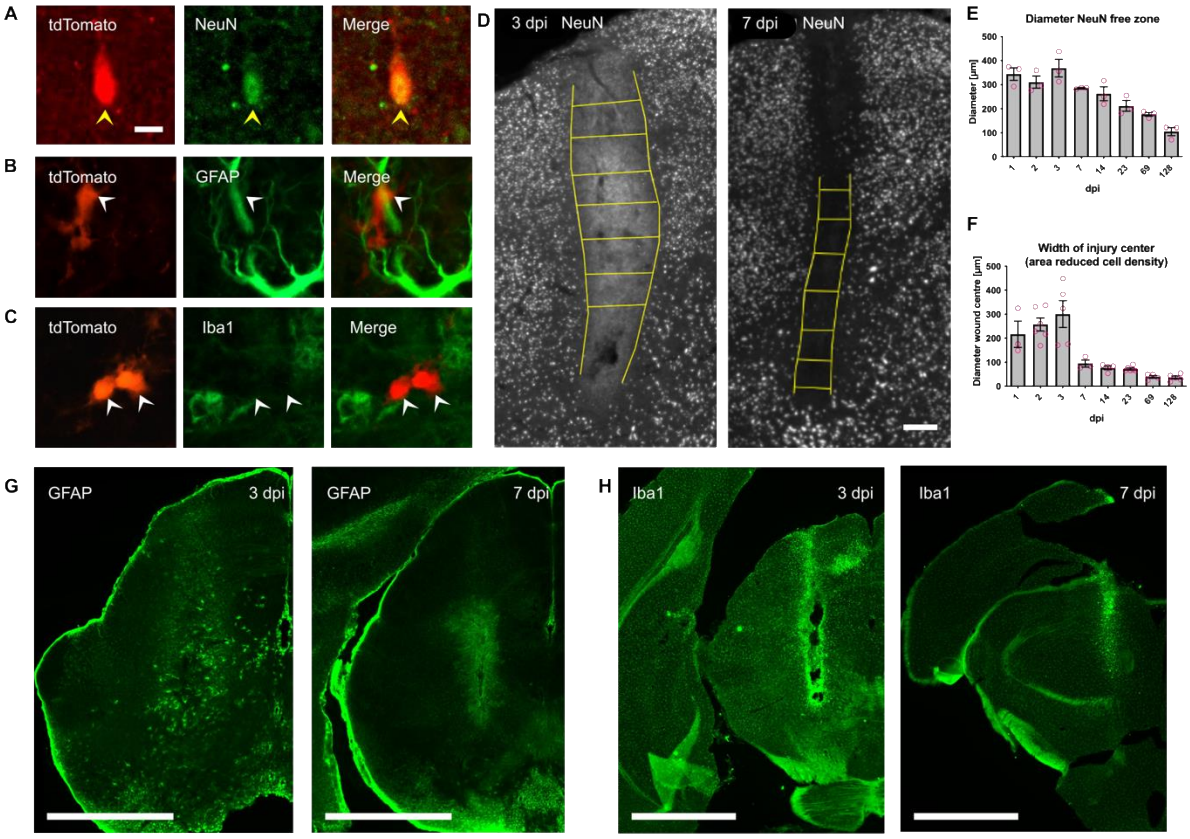

Figure S1: Identification of CRH-expressing cells at injury site. A-C, Immuno stainings for NeuN, GFAP and Iba1 at the injury site in *CRH-Cre::Ai9* mice, showing only co-localization of tdTomato with NeuN. **D**, Anti NeuN staining at 3 and 7 dpi in *CRH-Cre::Ai9* mice for injury size assessment. Scale bar, 50 µm. **E**, Diameter of NeuN free zone around injury core from 1 to 128 dpi. **F**, Width of wound center defined as an area with a decreased cell (DAPI) density between 1 and 128 dpi. **G-H**, Representative confocal image of anti GFAP (**G**) and Iba1 (**H**) staining at 3 and 7 dpi, scale bar, 1000 µm. For all images, White arrowheads indicate cells or structures. Yellow arrowheads indicate co-localization of two markers. All data are represented as mean +/- SEM.

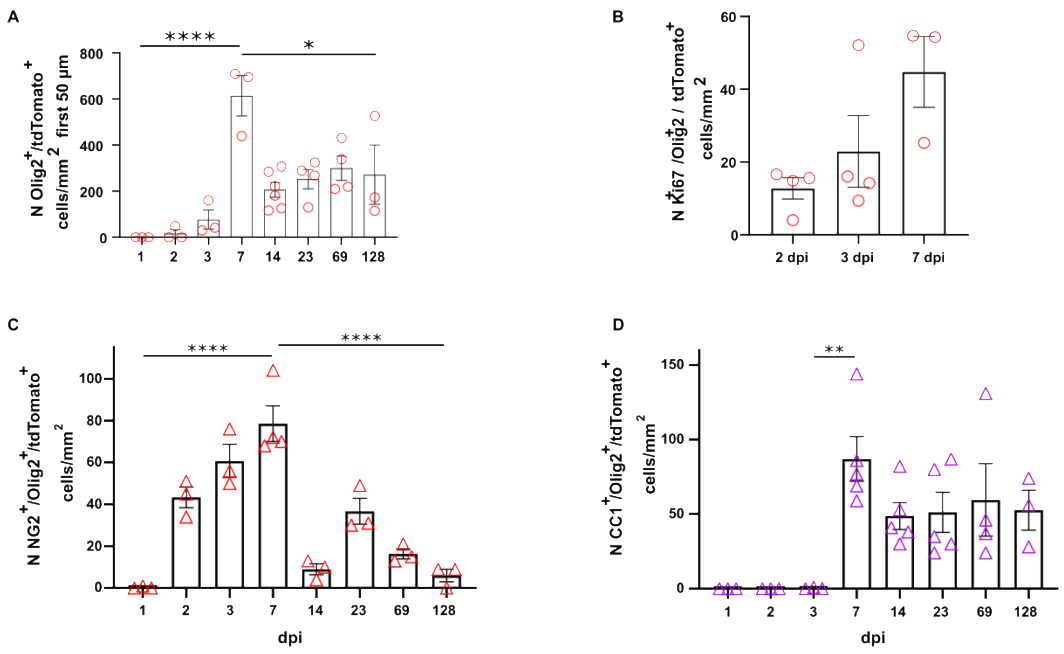

Figure S2: Population dynamics and proliferation of CRH$^+$ OPCs following acute injury. A, Quantification of Olig2$^+$/tdTomato$^+$ cells at ± 50 µm around the injury site. Changes were observed over time (One-way ANOVA: $F_{(7, 21)} = 10.27$, $p < 0.0001$) with an increase between 1 and 7 dpi (Bonferroni's post hoc test: ****$p < 0.0001$, 95% Confidence interval (C.I.) = -909.2, -318.7) followed by a decrease between 7 and 128 dpi (Bonferroni's post hoc test: *$p = 0.0158$, 95% C.I. = 47.3, 637.8). **B**, Quantification of Ki67$^+$/Olig2$^+$/tdTomato$^+$ cells/mm^2 at ± 300 µm around the injury site showing non-significant increase in the number of CRH-expressing Ki67$^+$ cells. n_{TP} = 3 - 4 mice. **C**, Quantification of NG2$^+$/tdTomato$^+$ cells/mm^2 at ± 300 µm around the injury site. Significant changes in cell numbers over time were observed (One-way ANOVA: $F_{(7, 17)} = 26.14$, $p < 0.0001$) with a significant increase between 1 and 7 dpi (Bonferroni's post hoc test: ****$p < 0.0001$, 95% C.I. = -106.9, -49.48) followed by a decrease between 7 and 128 dpi (Bonferroni's post hoc test: ****$p < 0.0001$, 95% C.I. = 43.81, 101.2). **D**, Quantification of CC1$^+$/tdTomato$^+$ cells/mm^2 at ± 300 µm around the injury site. Significant changes in cell numbers over time were observed (One-way ANOVA: $F_{(7,23)} = 5.186$, $p = 0.0012$ with a significant increase between 3 and 7 dpi (Bonferroni's post hoc test: **$p = 0.0081$, 95% C.I. = -158.4, -14.90) followed by a non-significant decrease. Between 14 and 128 dpi cell numbers were constant. n_{TP} = 3 - 5 mice. All data are represented as mean +/- SEM.

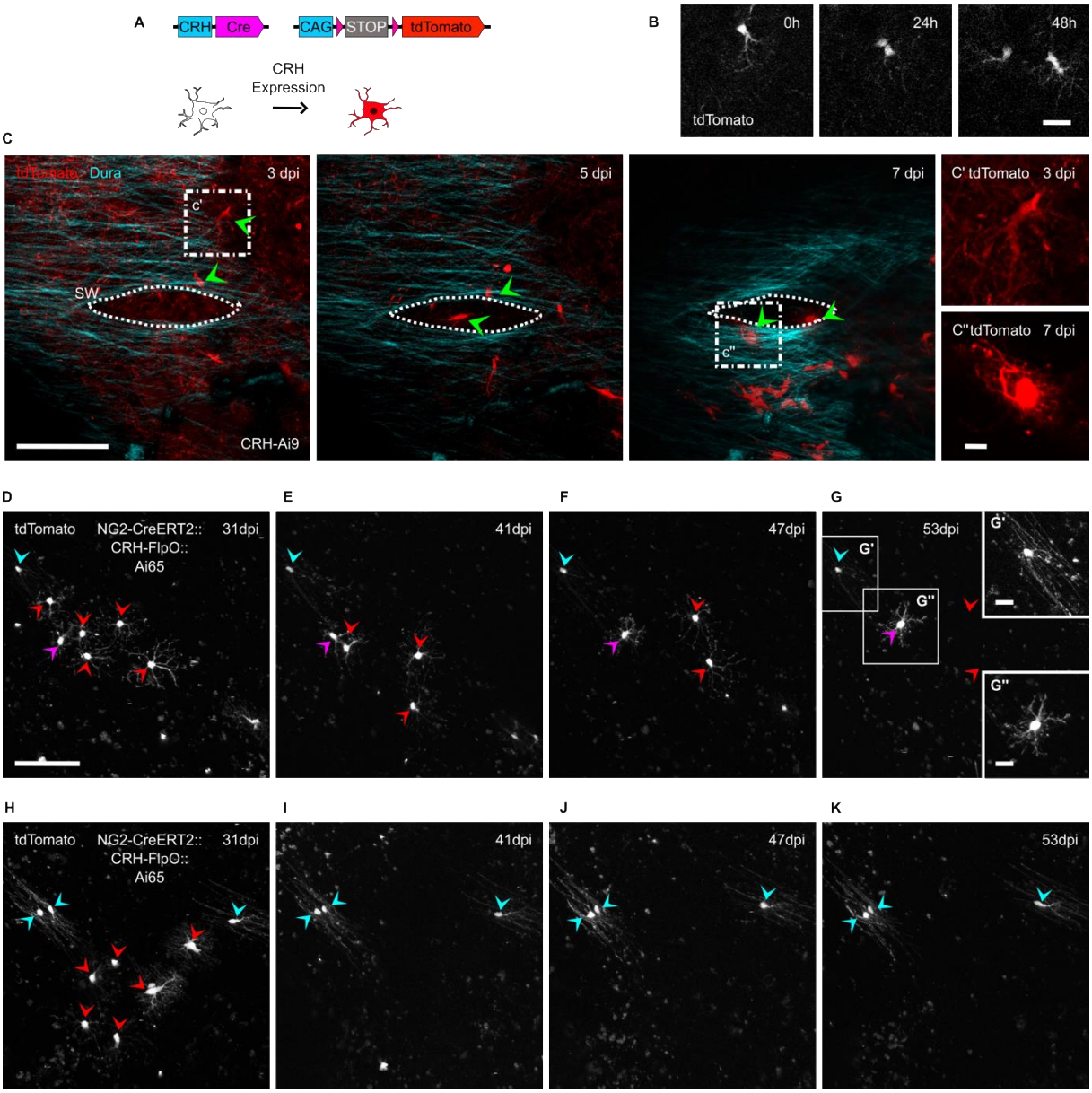

Figure S3: Stable integration is required for persistence of CRH-expressing OLCs. A, Graphical illustration of *CRH-Cre::Ai9* mouse model. **B,** 2-photon image of a proliferating tdTomato^{+} OPC in WM over the course of 48 h. Scale bar, 20 µm. **C**, Representative 2-photon images of a cortical injury (white lining: injury site in dura) between 3 and 7 dpi. Arrowheads (green) indicate cells moving towards wound center. Scale bar, 100 µm. **C'** and **C''**, morphological change of single cell between 3 and 7 dpi. Scale bar, 10 µm. **D-K**, 2-photon *in vivo* images of CRH-expressing OPCs after hippocampal cannula implantation at 31 (**D, H**), 41 (**E, I**), 47 (**F, J**) and 53 dpi (**G, K**) showing disappearance of immature premyelinating OLs with highly motile processes and growth cone like structures and long-lasting stability of mature OLs. For all images: red arrowheads indicate disappearing cells. Purple arrowhead indicates persisting cells. Cyan arrowheads indicate stable, myelinating OLs (as judged by morphology). Scale bars, 100 µm (overview), 20 µm (close up **G' and G''**). All data are represented as mean +/- SEM.

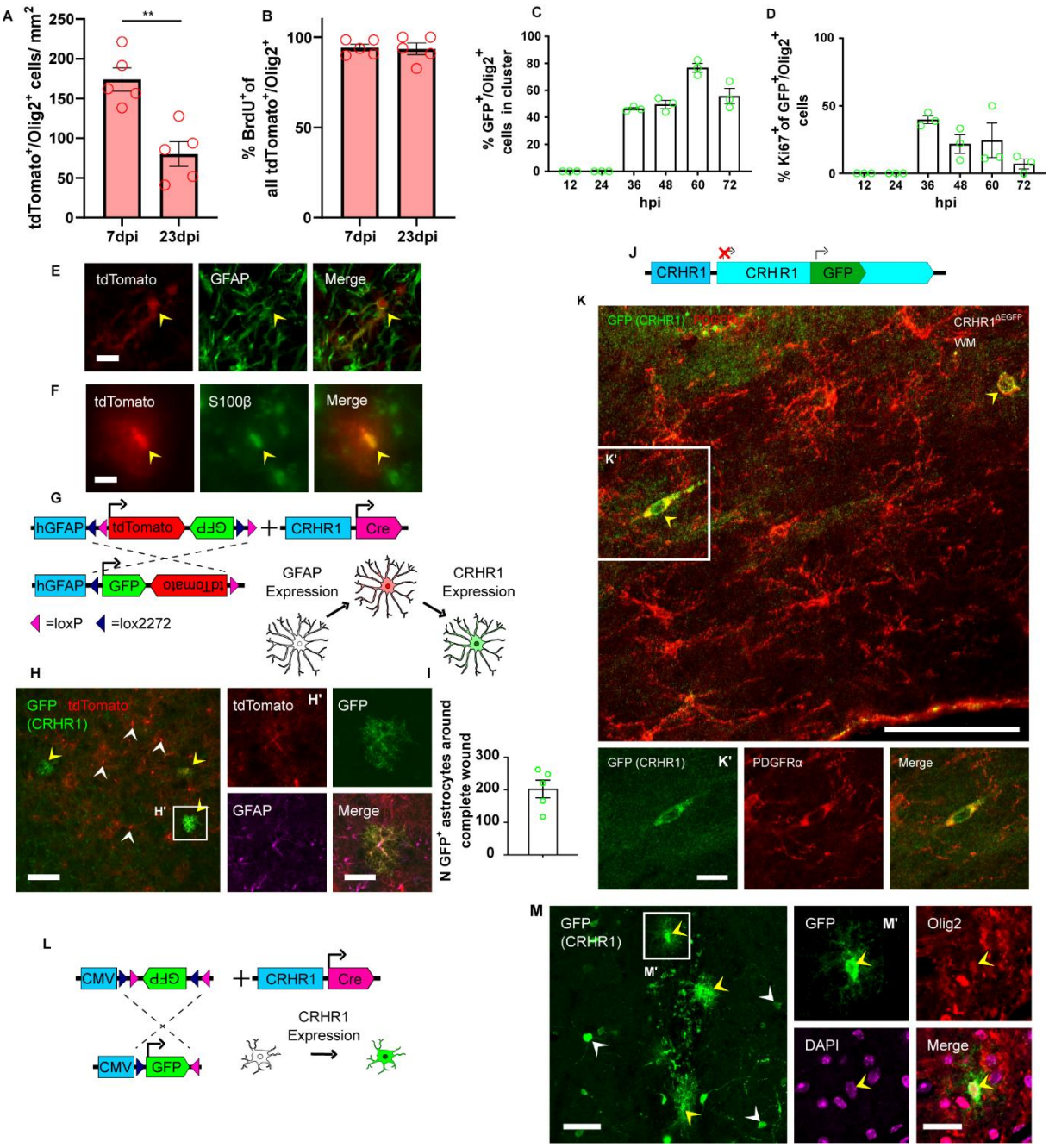

Figure S4: Characterization and quantification of CRHR1-expressing OLCs. **A**, Number of tdTomato$^+$/Olig2$^+$ cells/mm^2 in *CRH-Cre::Ai9* mice showing a significant decrease from 7 to 23 dpi (Welch's two-tailed t-test: $t_{(8)}$ = 4.399, **p = 0.0023, n_{TP} = 5 mice). **B**, Percentage BrdU$^+$ of all tdTomato$^+$/Olig2$^+$ cells in *CRH-Cre::Ai9* mice at 7 (94.225 ± 1.83) and 23 dpi (93.49 ± 3.24). **C**, Percentage of NG2$^+$/GFP$^+$ cells occurring in a multiplet of cells. n_{TP} = 3 mice. **D**, Quantification of Ki67$^+$ cells of all GFP$^+$/Olig2$^+$ cells. n_{TP} = 3 mice. **E,F** Confocal imaging of *CRHR1-Cre::Tau-LSL-FlpO::Ai9* mice revealed sparse GFAP (**E**) and S100β (**F**) stained tdTomato$^+$ astrocytes at injury site. Scale bar, 10 µm. **G**, Graphical illustration of injected AAV construct and *CRHR1-Cre* mouse line for the confirmation of CRHR1 expression in astrocytes. **H**, Overview of AAV injection site. Yellow arrow heads: GFP$^-$ (CRHR1$^+$) expressing cells. White arrow heads: tdTomato$^-$ (CRHR1$^-$) expressing

astrocytes. Scale bar, 100 µm. **H'**, Confocal image of tdTomato^{+}/GFP^{+}/GFAP^{+} astrocyte at injury site confirming co-localization of markers. Scale bar, 50 µm. **I**, Quantification of total number of GFP^{+}/tdTomato^{+}, GFP^{+}/tdTomato^{-} and all GFP^{+} astrocytes around the injury site. N = 6 animals. **J**, Graphical illustration of *CRHR1$^{\Delta EGFP}$* mouse model. **K**, GFP and PDGFRα co-staining in WM of *CRHR1$^{\Delta EGFP}$* mice showing CRHR1^{+}/PDGFRα^{+} cells. Scale bar, 100 µm (overview). 20 µm (close up **K'**). **l**, Graphical illustration of injected AAV construct and *CRHR1-Cre* mouse line for the confirmation of CRHR1 expression in OPCs. **M**, Overview of AAV injection site. Yellow arrow heads: GFP^{+} (CRHR1^{+}) expressing non-neuronal cells. White arrow heads: GFP^{+} (CRHR1^{+}) expressing neuronal cells. Scale bar, 50 µm. **M'**, Confocal image of GFP^{+}/Olig2^{+} OLC at injury site confirming co-localization of markers. Scale bar, 20 µm. For all images, White arrowheads indicate cells or structures. Yellow arrowheads indicate co-localization of two markers. All data are represented as mean +/- SEM.

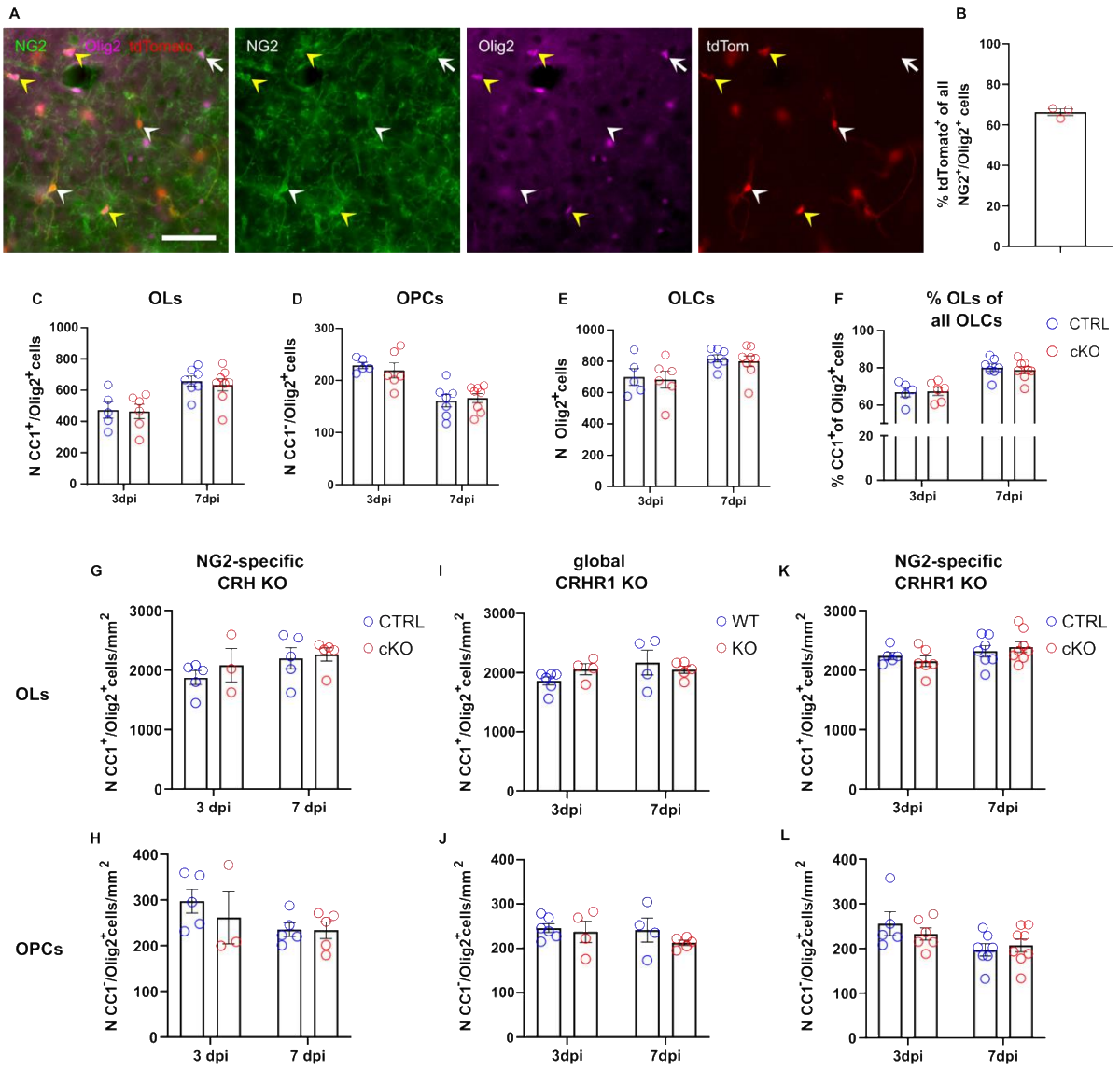

Figure S5: Characterization of injury site in LOF experiments. **A,** Representative image of tdTomato expression in NG2$^+$/Olig2$^+$ cells following TAM induction in NG2-specific CRH KO (*CRH$^{NG2\text{-}cKO}$*) animals showing effective Cre induction and consequent CRH KO. Scale bar, 50 µm. Arrowheads indicate recombined OPCs (tdTomato$^+$/NG2$^+$/Olig2$^+$) (yellow) and recombined pericytes (tdTomato$^+$/NG2$^+$/Olig2$^-$) (white), arrows (white) indicate not-recombined OPCs (tdTomato$^-$/NG2$^+$/Olig2$^+$). **B,** Quantification tdTomato$^+$ cells of all NG2$^+$/Olig2$^+$ cells showing a recombination efficiency of 66.3 ± 1.6 %. **C-F**, In NG2-specific CRHR1 KO mice no significant differences were detected between cKO vs CTRL animals with respect to the number of: CC1$^+$/Olig2$^+$ cells (Two-way ANOVA: time, $F_{(1,22)} = 17.77$, $p = 0.0004$, $n_{CTRL\ 3dpi} = 5$, $n_{cKO\ 3dpi} = 6$. $n_{CTRL\ 7dpi} = 7$, $n_{KO\ 7dpi} = 8$), CC1$^-$/Olig2$^+$ cells (Two-way ANOVA: time, $F_{(1,22)} = 29.79$, $p < 0.0001$), Olig2$^+$ cells (Two-way ANOVA: time, $F_{(1,22)} = 8.402$, $p = 0.0083$) and percentage of CC1$^+$ of all Olig2$^+$ cells (Two-way ANOVA: time, $F_{(1,22)} = 32.99$, $p < 0.0001$). **G-L**, Quantification of CC1$^+$/Olig2$^+$ (**G,I,K**) and CC1$^-$/Olig2$^+$ (**H,J,L**) in non-injured region of NG2-specific CRH KO (**G,H**), global CRHR1 KO (**I,J**) and NG2-specific CRHR1 KO (**K,L**) mice. Numbers for all populations are comparable between lines. $n_{TP/Group}$ = 3 - 8 mice. All data are represented as mean +/- SEM.

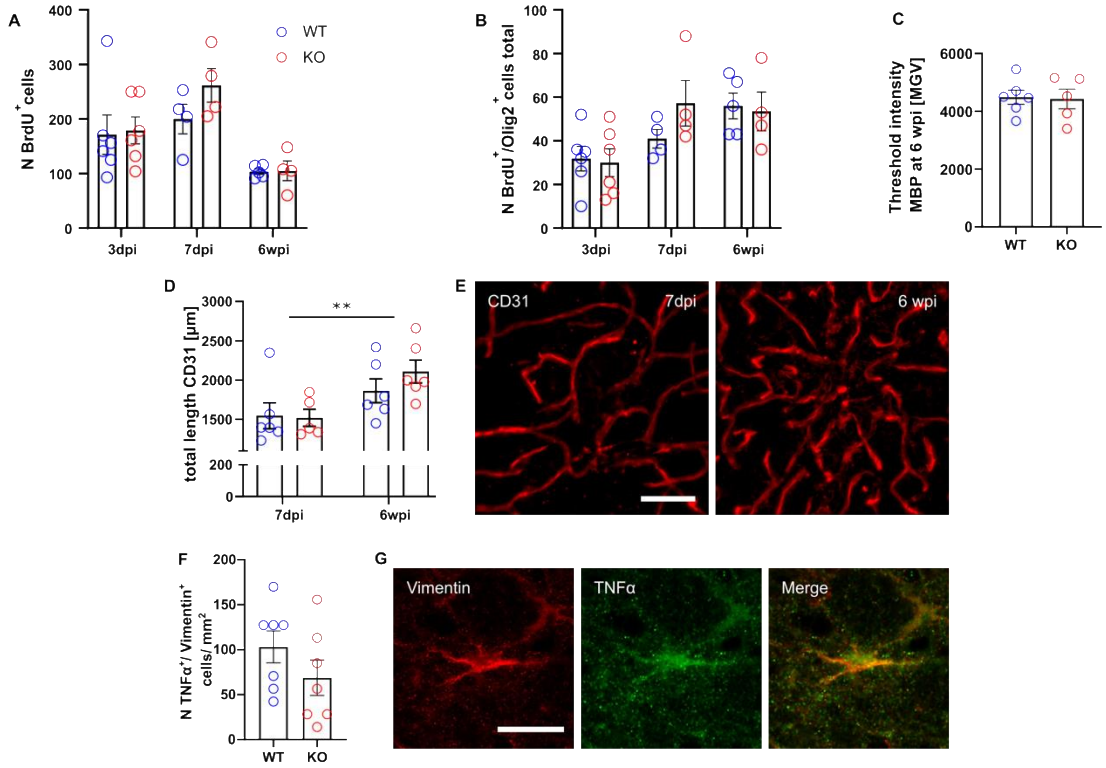

Figure S6: Quantification of all BrdU$^+$ cells and BrdU$^+$ OLCs following acute injury in *CRHR1$^{\Delta EGFP}$* animals. A-B, Quantification of BrdU$^+$ and BrdU$^+$/Olig2$^+$ cells in 300 µm radius around injury site at 3 dpi, 7 dpi and 6 wpi in *CRHR1$^{\Delta EFGP}$* animals showing no significant differences between WT and KO conditions. **C**, Mean grey value (MGV) of threshold analysis of MBP staining at injury site at 6 wpi. n = 5-6. **D**, Quantification of total length of CD31$^+$ vasculature around injury site at 7 dpi and 6 wpi showing significant increase over time without genotype effect (Two-way ANOVA: time, $F_{(1,19)}$ = 9.346, Sidak's post hoc test: **p = 0.0065; genotype, $F_{(1,19)}$ = 0.5439, p = 0.4699, $n_{WT\ 7dpi}$ = 6. $n_{KO\ 7dpi}$ = 5, $n_{WT\ 6wpi}$ = 6. $n_{KO\ 6wpi}$ = 6). **E**, Representative Confocal image of CD31 staining around injury site at 7 dpi and 6 wpi. Scale bar, 50 µm. **F**, Quantification of TNFα$^+$/Vimentin$^+$/mm^2 around injury site in *CRHR1$^{\Delta EFGP}$* animals at 3 dpi showing non-significant reduction in KO animals. N = 7 animals/genotype. **G**, Confocal images of Vimentin-TNFα co-staining showing co-expression of both markers. Scale bar, 20 µm. All data are represented as mean +/- SEM.

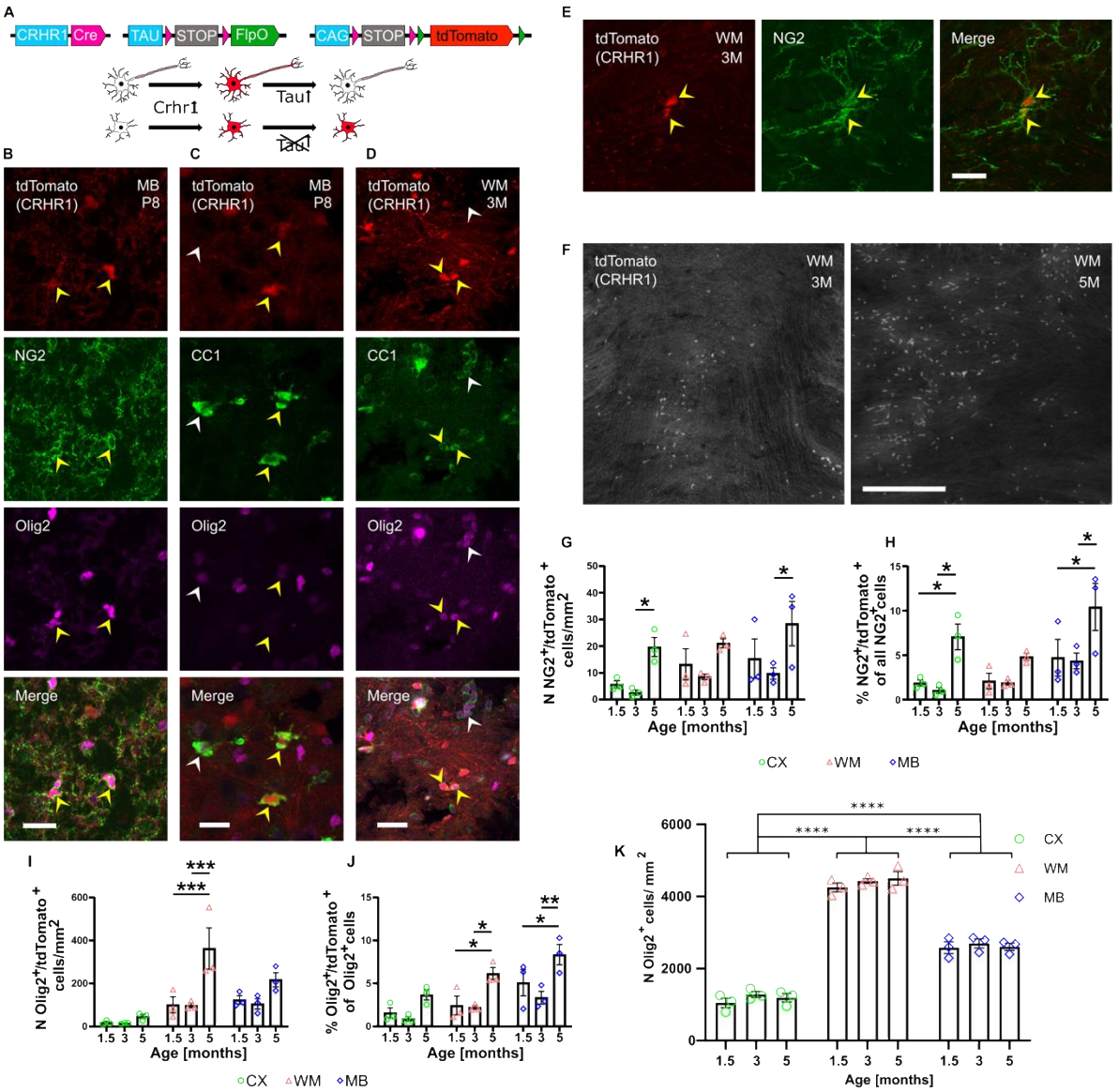

Figure S7: Quantification of CRH$^+$ and CRHR1$^+$ OLCs under non-injury conditions. A, *CRHR1::Tau-LSL-FlpO::Ai9* reporter mouse model. **B-E**, Confocal images showing co-localization of tdTomato (CRHR1) with NG2 and CC1 at P8 and at 3 months. Scale bar, 20 µm. **F**, Maximum intensity projections of confocal images of WM at 3 and 5 months of age. Scale bar, 200 µm. **G**, Quantification of NG2$^+$/tdTomato$^+$ cells at 1.5, 3 and 5 months of age in CX, WM and MB showing significant increase in CX and MB (Two-way ANOVA: time, $F_{(2, 18)} = 10.34$, $p = 0.001$, Sidak's post hoc test: *p = 0.044 (CX), *p = 0.025 (MB), $n_{TP} = 3$ mice). **H,** Percentage of NG2$^+$/tdTomato$^+$ of all NG2$^+$ cells showing significant increase over time (Two-way ANOVA: time, $F_{(2, 18)} = 13.46$, $p = 0.0003$, Sidak's post hoc test: *p = 0.034 (CX 1.5-5), *p = 0.012 (CX 3-5), *p = 0.0189 (MB 1.5-5), *p = 0.012 (MB 3-5), $n_{TP} = 3$ mice). **I,** Quantification of Olig2$^+$/tdTomato$^+$ cells at 1.5, 3 and 5 months of age in CX, WM and MB (Two-way ANOVA: time, $F_{(2, 18)} = 12.19$, $p = 0.0005$, Sidak's post hoc test: ***p = 0.0003 (WM 1,5-5), ***p = 0. 0003 (WM 3-5) $n_{TP} = 3$ mice). **J**, % Olig2$^+$/tdTomato$^+$ of all Olig2$^+$ cells in WM and MB (Two-way ANOVA: time, $F_{(2, 18)} = 16.65$, $p < 0.0001$, Sidak's post hoc test: *p = 0.0192 (WM 1,5-5), *p = 0.0129 (WM 3-5), *p = 0.041 (MB 1.5-5), **p = 0.002 (MB 3-5), $n_{TP} = 3$ mice). **K**, Quantification of Olig2$^+$ cells in CX, WM and MB at 1.5, 3 and 5 months of age shows no increase in the total number

of Olig2$^+$ cells. The number of Olig2$^+$ cells are significantly different between regions and highest in WM followed by MB and CX (Two-way ANOVA: region, $F_{(2,18)} = 480.2$, Sidak's post hoc test: ****$p < 0.0001$, $n_{TP} = 3$ mice). All data are represented as mean +/- SEM.

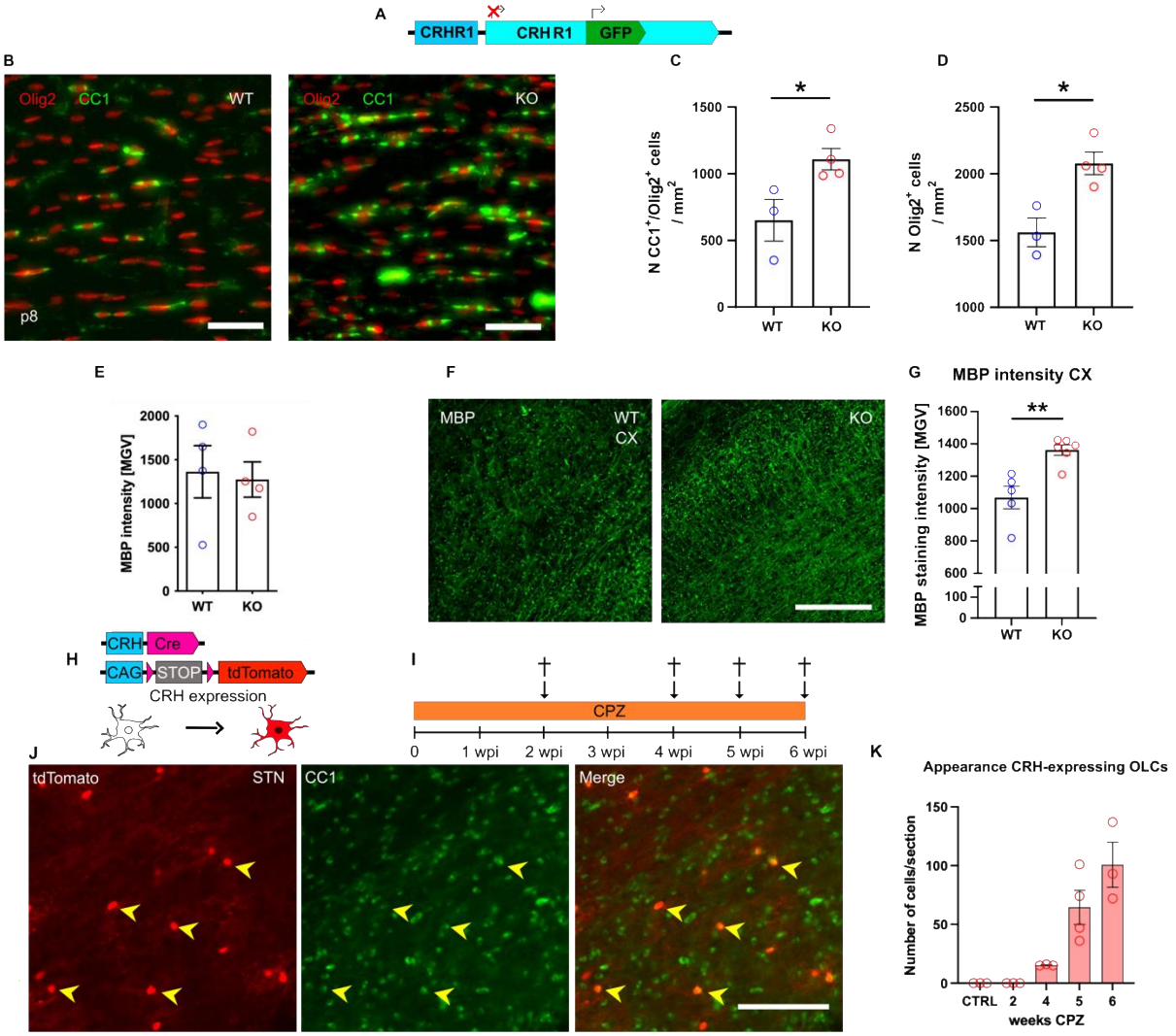

Figure S8: Impact of CRHR1 KO on OLC numbers and quantification of CRH⁺ OLCs following CPZ treatment. **A**, *CRHR1$^{\Delta EFGP}$* mouse model a *de facto* KO of CRHR1. **B**, Confocal images of CC1⁺/Olig2⁺ cells in CC of *CRHR1$^{\Delta EGFP}$* WT and KO animals at p8. Scale bar, 50 µm. **C** and **D**, Quantification of CC1⁺/Olig2⁺ (**C**) and all Olig2⁺ (**D**) cells/mm² in CC (Two-tailed Students t-test: $n_{CC1/Olig2}$: $t_{(5)} = 2.82$, *p = 0.037; n_{Olig2}: $t_{(5)} = 3.85$, *p = 0.012). **E**, Quantification of MBP intensity in lateral corpus callosum of *CRHR1$^{\Delta EGFP}$* mice at P8. **F**, Confocal image of MBP staining in CX of *CRHR1$^{\Delta EGFP}$* mice. Scale bar, 100 µm. **G**, Quantification of staining intensity of MBP in CX of *CRHR1$^{\Delta EGFP}$* mice (Two-tailed Students t-test: $t_{(9)} = 4.07$, **p = 0.0028; $n_{animals/condition}$ = 5-6). **H**, Graphical illustration of *CRH-Cre::Ai9* mouse model. **I**, experimental schedule for CPZ treatment of *CRH-Cre::Ai9* mice. **J**, Representative confocal image of CC1⁺/tdTomato⁺ cells in the subthalamic nucleus (STN) after 5 weeks of CPZ treatment. Scale bar, 50 µm. **K**, Quantification of CC1⁺/tdTomato⁺ cells after 2 to 6 weeks of CPZ treatment (One-way ANOVA: $F_{(4, 11)} = 3.704$, p = 0.0002). All data are represented as mean +/- SEM.

Table S1: Details of used mouse lines

Mouse line	Individual Mouse Lines	MGI Allele	MGI Identifier	Description/ Reporting
CRH-Cre::Ai9	*CRH-Cre* *Ai9*	*Crh*$^{tm1(cre)Zjh}$ *Gt(ROSA)26Sor*$^{tm9(CAG\text{-}tdTomato)Hze}$	MGI:4452089 MGI:3809523	tdTomato expression in CRH-expressing cells
NG2-CreERT2::Ai9	*NG2-CreERT2* *Ai9*	*Tg(Cspg4-cre/Esr1*)BAkik* *Gt(ROSA)26Sor*$^{tm9(CAG\text{-}tdTomato)Hze}$	MGI:4819178 MGI:3809523	tdTomato expression in NG2-expressing cells after induction by tamoxifen
CRH-Venus	*CRH-Venus*	*Crh*$^{tm1.1Ksak}$	MGI:6144041	Venus knock-in into *Crh* locus
CRH-FlpO::NG2-CreERT2::Ai65	*CRH-FlpO* *NG2-CreERT2* *Ai65*	*Crh*$^{tm1.1(flpo)Bsab}$ *Tg(Cspg4-cre/Esr1*)BAkik* *Gt(ROSA)26Sor*$^{tm65.1(CAG\text{-}tdTomato)Hze}$	MGI:6116854 MGI:4819178 MGI:5478743	tdTomato expression in CRH and NG2 co-expressing cells after induction by tamoxifen
CRH-FlpO::CRHR1-Cre::Ai65	*CRH-FlpO* *CRHR1-Cre* Ai65	*Crh*$^{tm1.1(flpo)Bsab}$ *Crhr1*$^{tm4.1(cre)Jde}$ *Gt(ROSA)26Sor*$^{tm65.1(CAG\text{-}tdTomato)Hze}$	MGI:6116854 MGI:6201420 MGI:5478743	tdTomato expression in CRH and CRHR1 co-expressing cells
CRH$^{NG2\text{-}cKO}$ (*CRH*^{loxP}*:: NG2-CreERT2::Ai9*)	*CRH*^{loxP} *NG2-CreERT2* *Ai9*	*Crh*$^{tm1.1Jde}$ *Tg(Cspg4-cre/Esr1*)BAkik* *Gt(ROSA)26Sor*$^{tm9(CAG\text{-}tdTomato)Hze}$	MGI:6201415 MGI:4819178 MGI:3809523	CRH knockout and tdTomato expression in NG2-expressing cells after induction by tamoxifen; tdTomato allowed quantification of recombination efficiency
CRHR1$^{NG2\text{-}cKO}$ (*CRHR1*^{loxP}*::NG2-CreERT2*)	*CRHR1*^{loxP} *NG2-CreERT2*	*Crhr1*$^{tm2.2Jde}$ *Tg(Cspg4-cre/Esr1*)BAkik*	MGI:5440013 MGI:4819178	CRHR1 knockout in NG2-expressing cells after induction by tamoxifen
CRHR1$^{\Delta EGFP}$	*CRHR1*$^{\Delta EGFP}$	*Crhr1*^{tm1Jde}	MGI:5294436	EGFP knock-in into *Crhr1* locus Global/constitutive CRHR1 knockout
CRHR1-Cre::Tau-LSL-FlpO::Ai9	*CRHR1-Cre* *Tau-LSL-FlpO* *Ai9*	*Crhr1*$^{tm4.1(cre)Jde}$ *pending* *Gt(ROSA)26Sor*$^{tm9(CAG\text{-}tdTomato)Hze}$	MGI:6201420 pending MGI:3809523	tdTomato expression in CRHR1-expressing cells; deletion of tdTomato expression in cells with high MAPT expression, enrichment of tdTomato expression in glial CRHR1-expressing cells

Table S1 continued: Details of used mouse lines

Mouse line	Individual Mouse Lines	MGI Allele	MGI Identifier	Description/ Reporting
CRHR1-Cre::Sun1-GFP	*CRHR1-Cre* *Sun1-GFP*	*Crhr1*$^{tm4.1(cre)Jde}$ *Gt(ROSA)26Sor*$^{tm5(CAG\text{-}Sun1/sfGFP)Nat}$	MGI:6201420 MGI:5443817	GFP expression in nuclear membrane of CRHR1-expressing cells
CRH-FlpO::Ai65F::CRHR1-Cre::Sun1-GFP	*CRH-FlpO* *Ai65F* *CRHR1-Cre* *Sun1-GFP*	*Crh*$^{tm1.1(flpo)Bsab}$ *Gt(ROSA)26Sor*$^{tm65.2(CAG\text{-}tdTomato)Hze/J}$ *Crhr1*$^{tm4.1(cre)Jde}$ *Gt(ROSA)26Sor*$^{tm5(CAG\text{-}Sun1/sfGFP)Nat}$	MGI:6116854 MGI:6260212 MGI:6201420 MGI:5443817	tdTomato expression in CRH-expressing cells and GFP expression in the nuclear membrane of CRHR1-expressing cells

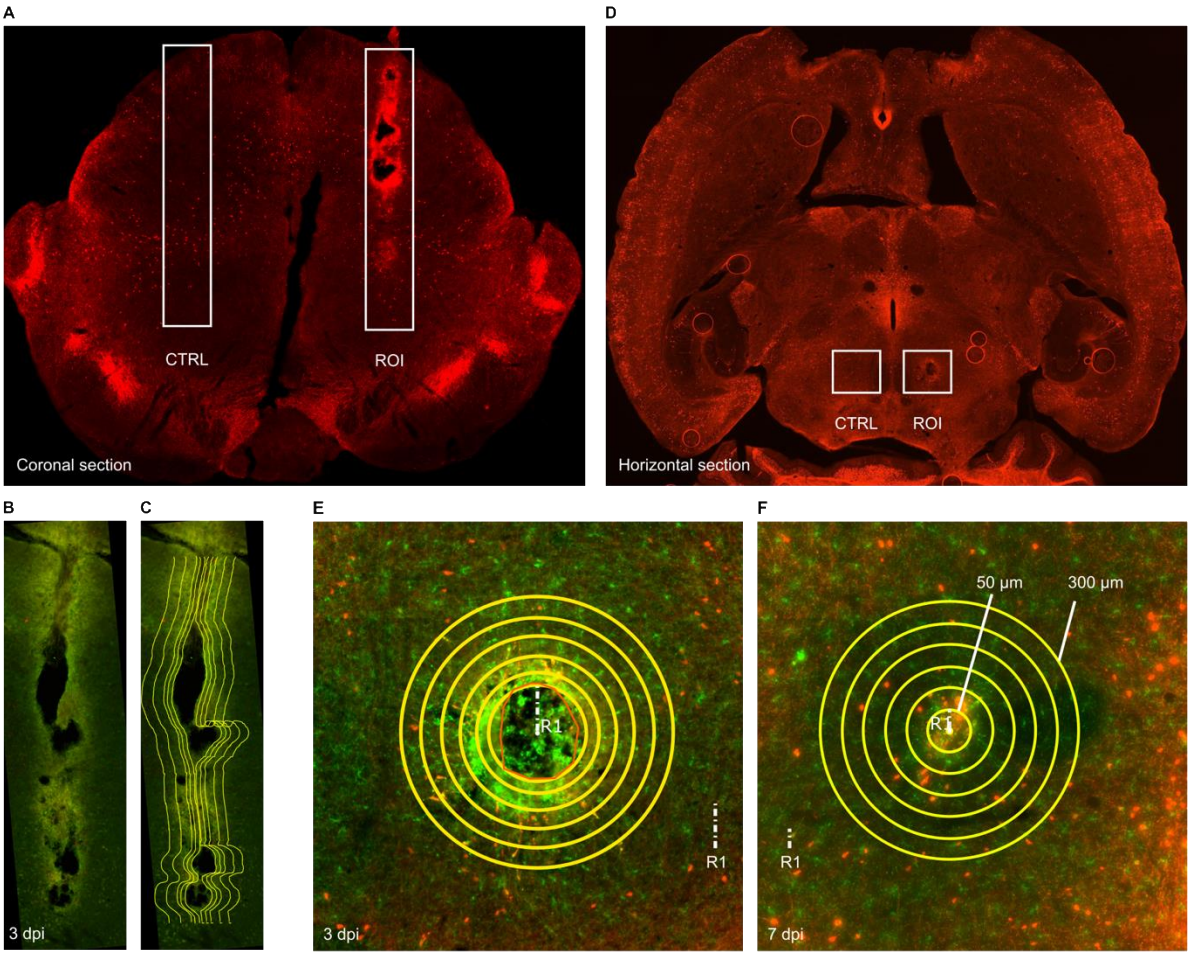

Method S1: Quantification matrices used for wound analysis. A, Coronal overview of acute injury in MB of *CRH-Cre::Ai9* mice. White squares: CTRL region and ROI around injury site. **B**, ROI around injury site. **C**, counting matrix generated automatically around center of wound. Subareas from 50 to 300 µm around injury site. **D**, Horizontal overview of acute injury in MB of *CRH-Cre::Ai9* mice. White squares: CTRL region and ROI around injury site. **E, F,** Quantification matrix at 3 dpi (**E**) and 7 dpi (**F**). Matrix consist of 6 circles with radii from 50 to 300 µm.

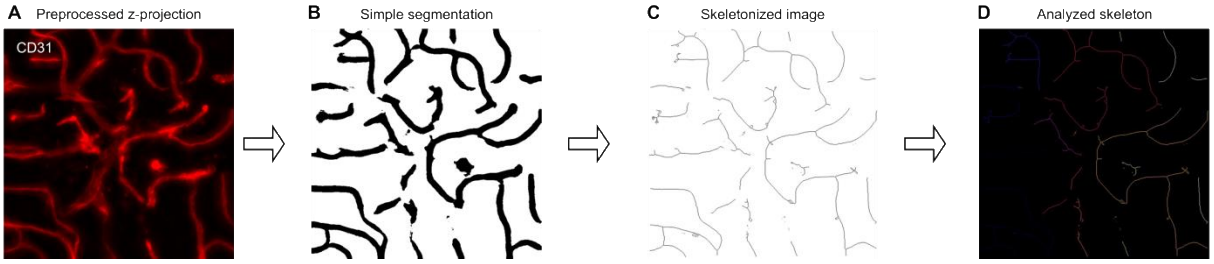

Method S2: Workflow of CD31^{+} vasculature quantification. A, Preprocessed image for analysis. **B,** Segmented image after processing by Ilastik**. C,** Skeletonized image processed with "Skeletonize (2D/3D)" function of Fiji. **D**, Analyzed skeleton application of Fiji built-in function "Analyze-Skeleton (2D/3D)".